arXiv:1101.5439v1 [cond-mat.mes-hall] 28 Jan 2011

Coulomb oscillations of the Fano-Kondo effect and zero bias anomalies in the double dot meso-transistor

A. Aldea[1,2], M. Ţolea[1], I.V. Dinu[1]

[1] *National Institute of Materials Physics, POB MG-7, 77125 Bucharest-Magurele, Romania.*

[2] *Institute of Theoretical Physics, Cologne University, 50937 Cologne, Germany.*

Abstract

We investigate theoretically the transport properties of the side-coupled double quantum dots in connection with the experimental study of Sasaki *et al.* Phys.Rev.Lett.**103**, 266806 (2009). The novelty of the set-up consists in connecting the Kondo dot directly to the leads, while the side dot provides an interference path which affects the Kondo correlations. We analyze the oscillations of the source-drain current due to the periodical Coulomb blockade of the many-level side-dot at the variation of the gate potential applied on it. The Fano profile of these oscillations may be controlled by the temperature, gate potential and interdot coupling. The non-equilibrium conductance of the double dot system exhibits zero bias anomaly which, besides the usual enhancement, may show also a suppression (a dip-like aspect) which occurs around the Fano *zero*. In the same region, the weak temperature dependence of the conductance indicates the suppression of the Kondo effect. Scaling properties of the non-equilibrium conductance in the Fano-Kondo regime are discussed. Since the SIAM Kondo temperature is no longer the proper scaling parameter, we look for an alternative specific to the double-dot. The extended Anderson model, Keldysh formalism and equation of motion technique are used.

PACS numbers: 73.23.-b, 73.63.-b, 73.63.Kv, 85.35.Ds

I. INTRODUCTION

The problem we address enter the family of effects resulting from the interplay of interference processes, Kondo correlations and Coulomb blockade in complex quantum dot systems. The specific mesoscopic set-up we study (shown in Fig.1) is a side-coupled double quantum dot with the small dot connected to external leads and also to a larger lateral dot. The set-up resembles the transistor structure, where the lateral big dot plays the role of the 'basis' and controls the current flowing from the left lead (the source) to the right lead (the drain).

The small dot is a "Kondo dot" containing one degenerate level E_d which is at most single occupied due to the strong Hubbard repulsion, and can be tuned in different regimes: Kondo, mixed valence or empty level. The side-dot contains many levels, and the access of the charge carriers into this dot is controlled by the Coulomb blockade which can be periodically switched on/off by a continuous variation of the gate potential V_g. In this way the interference conditions in the device can be changed periodically resulting in a periodical modulation of the source-drain conductance. The modulation will have a Fano shape which depends on the inter-dot coupling and the regime of the small (central) dot, which may work in Kondo or non-Kondo mode.

We have two motivations for considering a "large" side-coupled dot. First, because the electronic correlations are much weaker in a large dot, and, this way, the side-coupled dot basically provides just an interference path as considered by Sasaki *et al.* [1] in a recent experiment that motivated our work. The interesting physics arises from the fact that the interference occurs during the Kondo tunneling and the Kondo correlations are also affected. The second reason is that a large dot has small level spacing which can influence the shape of the Fano resonances.

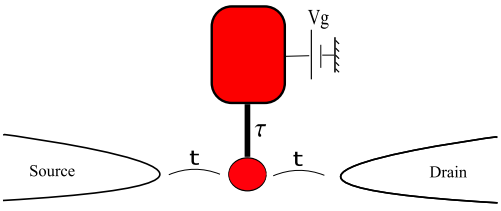


FIG. 1: (color online) The sketch of the transistor-like double dot system

The side-coupled double dot system has been much studied in the recent literature, and

various aspects has been put forward. The two-stage Kondo effect was proven if the two quantum dots are small and the spin screening takes place in both of them [2, 3]. The interplay between Fano and Kondo processes, known as Fano-Kondo effect, is specific to such a geometry. Wu *et al.* [4] studied the simple T-shape model which includes a single energy level in each dot. The slave-boson mean field theory (used at low bias and zero temperature) indicates the absence of the unitary limit of the linear conductance and also the suppression of the zero bias (peak-type) anomaly when the side dot is coupled. Recently, as already mentioned, Sasaki *et al.* [1, 5] investigated experimentally the linear conductance as function of the gate on the lateral dot, both in the Kondo and non-Kondo regime of the dot connected to leads. One proves the suppression of the Kondo effect by Fano destructive interferences. The finding is supported by a calculation in the slave-boson approximation again for the simple T-shape model, where the interference takes place between the resonant channel passing through the side-dot and the continuous Kondo channel (see also [6]). The problem is reassumed by Zitko [7] who suggests that the experiments in [1] may be also understood in the frame of a two stage Kondo effect if the experimental temperature lies between the two Kondo temperatures. The influence of ferromagnetic leads in the presence of an exchange between the two dots is studied in [8].

The non-equilibrium regime of quantum dot devices raises the question of the so-called zero bias anomaly (ZBA), consisting in a singular behavior of the differential conductance dI/dV at $V = 0$. ZBAs occur in various physical systems like semiconductor impurity bands [9], tunnel junctions [10] or quantum dots. For instance, the dip of the differential conductance found in metal-insulator-metal tunneling is attributed to the dip in the density of states of the electrodes. An elaborate theory due to Altshuler and Aronov proves that the disorder gives rise to such an effect if accompanied by electron-electron interaction. So, such anomalies are considered as a fingerprint of the Coulomb interactions.

ZBAs are present also in mesoscopic systems, as for instance, the strong maximum of the differential conductance observed in quantum dots below the Kondo temperature; the maximum is understood as corresponding to the Kondo-peak in the density of states of the dot (see for instance [11, 12]). The interaction is again a necessary ingredient, however, as a difference from the case of the tunneling junction mentioned above, the interaction occurs now inside the dot, and the information of interest is carried by the density of states of the dot, while the lead spectrum is described by the simple flat band model. Since the

experiment observes the suppression of the Kondo resonance due to destructive interference [1] one may ask whether the peak-type anomaly might not be replaced by a dip-type anomaly under specific conditions in double-dot systems. This question is one of the topics of the paper.

The scaling properties of the non-equilibrium conductance is a topic of present interest in the field, most papers addressing the single impurity Anderson model, e.g. [13–18]. In this paper we perform a scaling analysis of the nonequilibrium conductance $G = dI/dV$ of the transistor-like device based on double lateral dots connected to source and drain. We use the data collapse technique, i.e. we look for that scaling of $\Delta G(V,T) = G(0,T) - G(V,T)$ and of the variables V, T, T_K which produces the collapse of all numerical curves in a single one. The specific situation consists in the dip-peak crossover which means the change of sign of the curvature at the variation of the parameters V_g or T. This makes impossible the collapse of all curves in a single one, i.e. prevents the identification of a single -universal- scaling law. We succeed to prove scaling properties in the peak-like regime, the scaling parameter being the half-width of the Kondo peak for the double dot system.

The model we adopt is an extended Anderson Hamiltonian (see eq.(1)), and the conductance is calculated in the Keldysh formalism. Being interested not only in the Kondo but also in the mixed-valence regime, we shall use the equation of motion technique, which works well also in this case. In Sec.II we describe the model and the formalism. Sec.III analyzes the spectral properties of the specific double dot model. In Sec.IV we calculate the source-drain current versus the gate potential applied on the big dot. The oscillatory behavior and Fano aspect of the resonances are pointed out. Sec.V proves the peak-dip crossover of the zero bias anomaly in the transistor-like system and discusses some scaling properties of the nonequilibrium conductance.

II. THE MODEL HAMILTONIAN AND TRANSPORT FORMALISM

The set-up discussed in introduction will be described by the following Hamiltonian , which may be considered as an extended Anderson model:

$$H = \sum_{k,\sigma,\alpha} (\epsilon_k - \mu_\alpha) c^\dagger_{k\sigma,\alpha} c_{k\sigma,\alpha} + \sum_\sigma E_d d^\dagger_\sigma d_\sigma + U_H n_{d\uparrow} n_{d\downarrow} + \sum_{i\sigma} E_i c^\dagger_{i\sigma} c_{i\sigma} + \frac{e^2}{2C} N^2$$

$$+\sum_{k,\sigma,\alpha} t_{kd}\big(c^{\dagger}_{k\sigma,\alpha}d_{\sigma}+h.c.\big)+\sum_{i}\tau_{id}\big(c^{\dagger}_{i\sigma}d_{\sigma}+h.c.\big), \tag{1}$$

where one may identify the Hamiltonian of the leads ($\alpha = L(left), R(right)$), the Hamiltonian of the small dot including the Hubbard term, and that one of the big (lateral) dot which contains also the Coulomb repulsion in the orthodox (capacitance) model; the operator of the total occupation number reads $N = \sum_{i\sigma} n_{i\sigma} = \sum_{i\sigma} c^{\dagger}_{i\sigma}c_{i\sigma}$. The last two terms stand for the coupling of the small dot to the leads and to the big dot. Without loss of generality, the energy levels of the big dot will be treated as equidistant $E_i = E_0 + i\delta E \;\; (i = 0, 1, 2..)$; We notice that the Hamiltonian (1) reduces either to the usual SIAM when $\tau = 0$ or to the simple T-shape model when only one level is considered in the lateral dot. The term describing the Coulomb interaction in the big dot will not be taken explicitly into the formalism, however we shall keep in mind that, due to the Coulomb blockade, the charging energy required for absorbing any new electron in the big dot equals the quantity $\Delta = U_c + \delta E;\; U_c = e^2/C$.

The charge current flowing through the device is given in the Keldysh formalism by the well-known formula [19]:

$$I(V) = \frac{e}{\hbar}\sum_{\sigma}\int d\omega[f_L(\omega - \frac{eV}{2}) - f_R(\omega + \frac{eV}{2})]\;\Gamma_{\sigma}(\omega)[-\frac{1}{\pi}\;ImG^{r}_{dd,\sigma}(\omega)], \tag{2}$$

where the main ingredient is the retarded Green function $G^{r}_{dd,\sigma}$ at the site 'd' denoting the small dot. (V is the applied bias, Γ describes the coupling of the small dot to the leads, and $f_{L/R}$ are the Fermi functions on the left/right side). If we are not too far from equilibrium (i.e., $eV/kT << 1$), one may neglect the derivative of Γ and G^{r}_{dd} with respect to V, and the differential conductance reads (see also [13]):

$$G(V) = dI/dV = \frac{e^2}{2h}\sum_{\sigma}\Gamma_{\sigma}\;[ImG^{r}_{dd,\sigma}(-\frac{eV}{2}) + ImG^{r}_{dd,\sigma}(\frac{eV}{2})] \tag{3}$$

The above equation says that, for the system we take into consideration, the whole information about the possible zero-bias anomaly of the differential conductance is contained in the density of states of the small dot $DoS_d(\omega) = -\frac{1}{\pi}ImG_{dd}(\omega)$, which should be calculated in the presence of all couplings and interactions. Since the first derivative of $G(V)$ vanishes at $V = 0$, the zero-bias behavior is given by the second derivative (convexity) of the function $G(V)$ which is proportional to the convexity of the spectral function at the site 'd'. Indeed, in the absence of the spin dependence, one has:

$$G"(0) = -\frac{e^4}{h}\Gamma ImG"_{dd}(0). \tag{4}$$

This expression shows that an eventual change of the spectral function convexity yields a peak-dip crossover of the differential conductance.

For the calculation of the Green function we use the recipe proposed by Entin-Wohlmann et al [20] which is an extension to complex mesoscopic structures of the Lacroix equation of motion approach, originally used for SIAM [21]. The further extension of the formalism to non-equilibrium is described in [22]. The input quantity required by this recipe is the non-interacting self energy $\Sigma_0(\omega)$ (calculated in the absence of the Hubbard term in the small dot, $U_H = 0$). In order to identify this quantity in the case of the Hamiltonian (1), we sketch below the equations of motion of the Green functions specific to this problem:

$$(\omega^+ - E_d)G_{dd\sigma} = 1 + \sum_{k,\alpha} t_{dk} G^{\alpha}_{kd\sigma} + \sum_i \tau_{di} G_{id} + U_H \ll d_\sigma n_{d,-\sigma}; d^\dagger_\sigma \gg \tag{5}$$

$$(\omega^+ - \epsilon_k + \mu_\alpha)G^{\alpha}_{kd} = t_{kd} G_{dd}$$

$$(\omega^+ - \epsilon_i)G_{id} = \tau_{id} G_{dd}.$$

Combining the above equations, one obtains:

$$\big(\omega^+ - E_d - \Sigma_0(\omega)\big)G_{dd}(\omega) = 1 + U_H \ll d_\sigma n_{d,-\sigma}; d^\dagger_\sigma \gg . \tag{6}$$

This is a well known formula , however for our specific lateral double-dot model, Σ_0 includes two terms coming from the leads and the big dot, respectively:

$$\Sigma_0(\omega) = \sum_{k,\alpha} \frac{|t_{kd}|^2}{\omega^+ - \epsilon_k + \mu_\alpha} + \sum_i \frac{|\tau_{id}|^2}{\omega^+ - E_i}. \tag{7}$$

One notices that the two contributions are additive and both of them acts on the Kondo peak of the density of states of the small dot. The second term is that one which gives rise to the *Kondo in a box* effect, which was studied in [25] in the case of vanishing dot-leads coupling. In the simple description of the flat continuous spectrum for the leads the first term in eq.(7) equals $i\Gamma$ (the quantity present in the current formula eq.(2)). On the other hand, the second term in eq.(7) is a finite sum over the discrete spectrum of the big dot. This contribution can be tuned by the lowest energy level E_0, which will be identified from now on as the gate potential applied on the big dot, $E_0 \equiv V_g$ (see Fig.1).

III. THE SPECTRAL FUNCTION $ImG_{dd}(E)$

The spectral properties help with the identification of various possible regimes in the transport phenomena. Since the gate potential V_g applied on the big dot is the functional parameter of double dot device that works like a meso-transistor, the spectral function will be studied for different values of V_g. An analytical expression is available in the non-interacting case $U_H = 0$, showing properties which are also useful for the discussion of the numerical curves obtained in the presence of the interaction. From eqs.(6-7) one gets:

$$G^0_{dd}(\omega) = \big(\omega^+ - E_d + i\Gamma - \tau^2 \sum_i \frac{1}{\omega^+ - E_i}\big)^{-1} \tag{8}$$

and also the following expression for the imaginary part:

$$-\, ImG^0_{dd} = \frac{A^2(\omega)\Gamma}{[(\omega - E_d)A(\omega) - \tau^2 B(\omega)]^2 + A^2(\omega)\Gamma^2}, \tag{9}$$

where $A(\omega) = \Pi_i(\omega - E_i)$ and $B(\omega) = dA(\omega)/d\omega$ with $E_i = V_g + i\Delta$ (i = integer). The

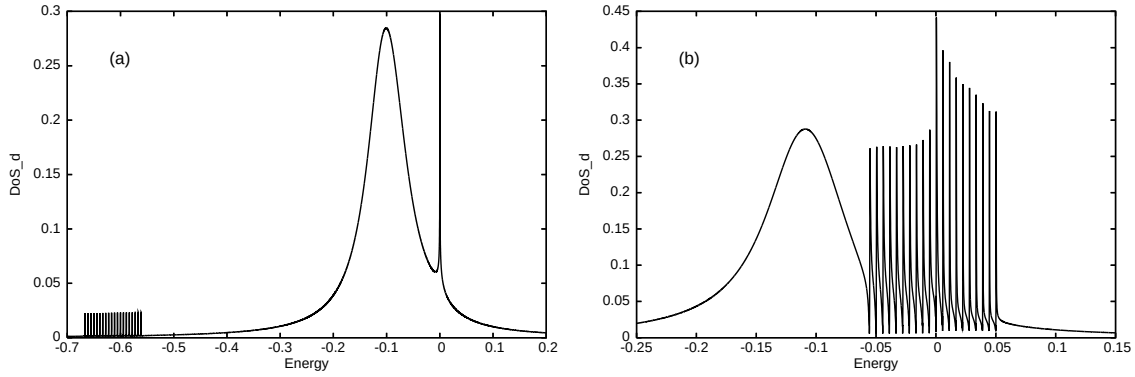


FIG. 2: The local density of states at the site d as function of energy for two values of the gate potential: (a) $V_g = -0.66$; (b) $V_g = -0.05$ ($E_d = -0.1$; the energy unit is the half-width of the leads band)

eq.(10) indicates that when $\tau \neq 0$ the spectral function has a series of equidistant zeros at $\omega = E_i$. This structure was noticed also by Liu [6]. The spectral function shows a specific structure, namely, besides the usual d-resonance, it exhibits a series of peaks located between the mentioned zeros .

In the interacting case ($U_H \neq 0$) , the Kondo effect arising in the small dot superimposes its own characteristics on the spectral function of the double-dot system. More than this, by changing the gate potential V_g one may choose different regimes. For instance, when

the gate is such that the bunch of levels $\{E_i\}$ is positioned much below the d-level E_d the local density of states at the d-level $DoS_d = -\frac{1}{\pi} ImG_{dd}$, looks as expected (see Fig 2a): the strong d-resonance carrying the Kondo peak at $E = E_f = 0$ is the most evident, while the oscillations coming from the hybridization with the big dot can be noticed at much lower energies. The density of states changes drastically if we push up the gate V_g such that the spectrum of big dot encompasses the Fermi energy; in this case the big dot (which is now only partially filled) becomes strongly hybridized with the small dot.

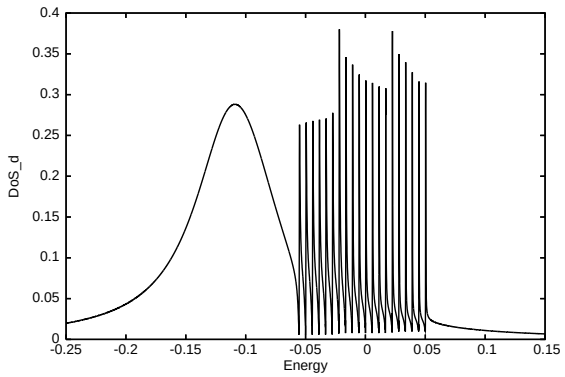


FIG. 3: The same as in Fig.2b in the presence of a bias $V = 0.04$

In the absence of the leads, the changes induced by the presence of the big dot to the density of states at the site d is known as 'the Kondo in a box' effect. Refs.[24–26] evidentiate oscillations of DoS_d due to finite size of the big dot, and also the presence of Kondo-type correlations which manifest itself in an increased spectral weight. In our system, despite the fact that the device is connected to infinite leads, we find an increase of the spectral weight above the Fermi energy (see Fig.2b). One may ask how the density of states looks in the case of an applied bias larger than the level spacing. It is well-known that a finite bias yields the splitting of the Kondo resonance of a single dot [19], however our interest concerns the double-dot system in the strong hybridization regime. The numerical result shows a two-step behavior: a first increasing step occurs at $-V/2$ followed by a second one at $+V/2$ as in Fig.3. In the next section we shall analyze the equilibrium conductance as function of V_g.

IV. THE FANO PROFILE OF THE COULOMB OSCILLATIONS OF THE SOURCE-DRAIN CONDUCTANCE

Our aim is to model the experimental device of Sasaki at al [1] and to analyze the output of the interplay between the Fano and Kondo effects in the double-dot transistor-like system. The source-drain current is the result of combined action of two channels: i) the resonant channel passing through the big dot (controlled by V_g) and ii) the Kondo channel through the small dot (controlled by Γ and temperature). The charge carrier may enter the big dot any time the gate potential compensates the charging energy $\Delta = U_c + \delta E$, where U_c is due to the Coulomb repulsion and δE is the distance between the levels of the big dot. In other words, the resonant channel is activated/deactivated periodically with V_g due to the periodical blockade of the big dot.

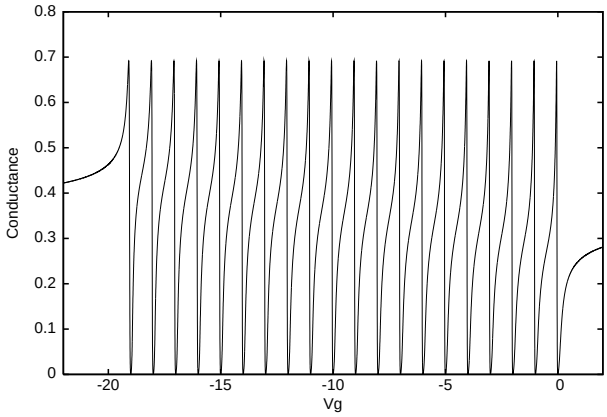


FIG. 4: The oscillations of the source-drain linear conductance when the gate on the big dot V_g is varied continuously. V_g is measured in units Δ and the number of levels in the big dot is $N = 20$. The small dot is in the Kondo regime: $E_d = -0.2, \Gamma = 0.04$ (measured in the leads band width), $T/T_K = 1/10$.

On the other hand, the device is typical for the occurrence of the Fano effect. When the gate on the big dot is changed continuously, the Fano interference gives rise to Fano lines which repeat in a sequence with the Coulomb blockade periodicity Δ. Denoting by γ the width of the Fano resonance, the ratio γ/Δ is responsible for the general aspect of the sequence, as it controls the degree of overlapping of neighboring resonances. When this ratio is small enough the resonances are independent and the usual Fano expression holds

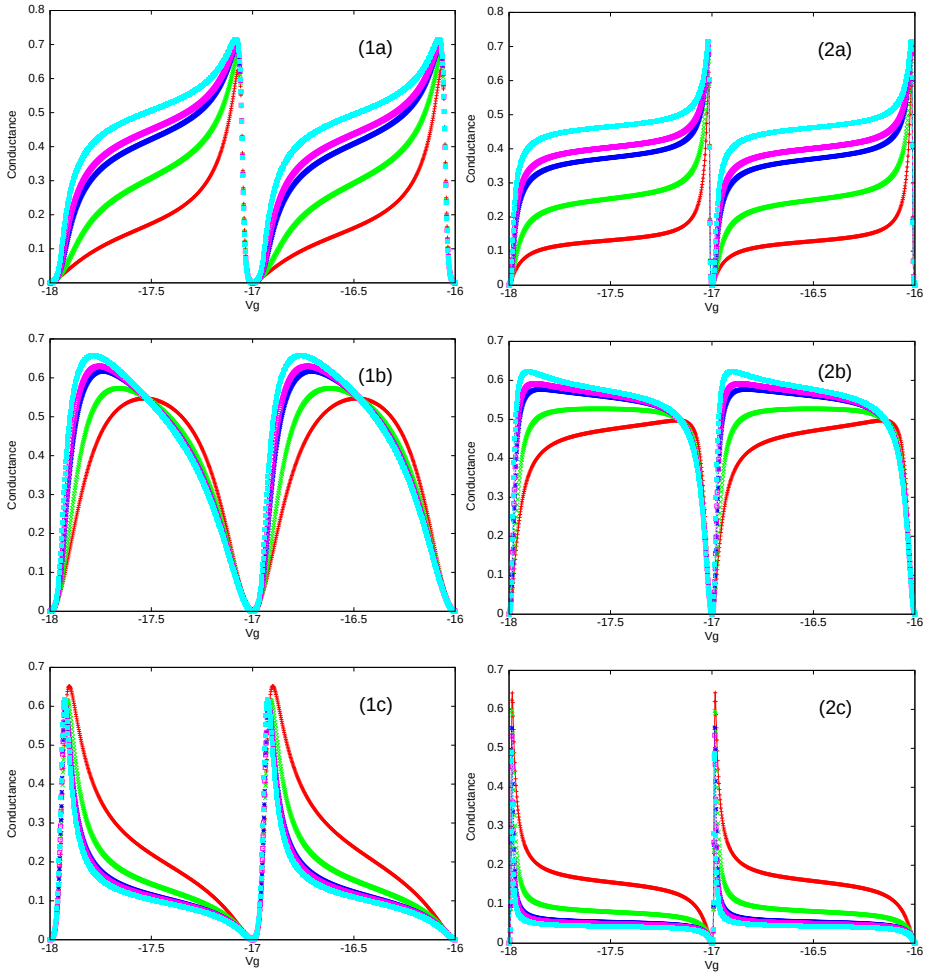


FIG. 5: (color online) Two periods of the oscillations shown in Fig.4 for two values of the inter-dot hybridization $\tau = 0.01$ (left) and $\tau = 0.005$ (right). At smaller τ the Fano resonance is narrower and the background more evident. One notices the differences in the temperature dependence of the oscillation amplitude : in the Kondo regime (panels 'a') the conductance decreases with increasing temperature, the opposite occurs in the empty level (panels 'c'), but a visible crossing of the isotherms occurs in the mixed valence regime (panels 'b'). (The red curves denote the highest temperature).

around each resonance:

$$G(\epsilon) = const\frac{(\epsilon + q)^2}{\epsilon^2 + 1}, \quad \epsilon = \frac{E - \epsilon_0}{\gamma/2}, \tag{10}$$

(where ϵ_0 is the resonance energy , q is the Fano asymmetry factor and the constant gives

the background value).

The equilibrium source-drain conductance, for a large range of V_g, is shown in Fig.4, while Fig.5 shows two periods of the Fano oscillations for the three specific regimes of the small dot: Kondo, mixed valence and empty level. The two columns correspond to different values of the coupling parameter τ which controls the resonance width. It may be observed that small τ (the case in the right column) means a narrow resonance, in which case the background plateau becomes more evident.

The calculation is based on eq.(3) in the limit $V = 0$ and is performed at different temperatures. The upper panel evidentiates the increase of the conductance with decreasing temperature which is the typical effect of the Kondo correlations on the Fano lines, known as the Fano-Kondo effect. The lowest panel describes the empty level regime of the small dot where the temperature dependence is reversed compared to the Kondo regime, and the shape of the curves indicates also the change of the sign of the Fano asymmetry factor q. The asymmetry factor can be easily calculated in the non-interacting case ($U_H = 0$) and equals $q = E_d/\Gamma$, indicating that the sign of q is negative when the d-level lies in the well and positive when E_d is above the well. For the interacting case an analytical expression of q is not available, however the numerical results in Fig.5 show that the same change of sign holds when moving from the Kondo to empty level regime.

The crossover between the two extreme situations is shown in the middle panel which describes the mixed-valence regime. The significant issue is the presence of crossing points of the isotherms where $dG/dT = 0$. The most visible crossing occurs in the panel (1b) : one notices that to the right of the crossing point the conductance increases with the temperature (as in the empty level case), while to the left the dependence is opposite (similar to the Kondo regime). Such crossing points are present also in the cases (a) and (c), but they are very close to the Fano zero, and are not visible in Fig.5.

The analytical expressions of the conductance (extended formulae for complex meso-systems in the Lacroix's approximation [21] are given in [20]) are too cumbersome to evidentiate the crossing points, so we have to confine ourselves to numerical studies. However, because of the competition between the interference and Kondo effect, the change of the temperature behavior is understandable for the double dot device. Indeed, although the Kondo channel is reinforced with decreasing temperature, its superposition with the resonant channel may give rise to a destructive interference which results in a reduction of the

conductance when the temperature is decreased. A similar property has been found for the triangle interferometer with magnetic impurity [23].

Finally, we note that if V_g applied on the big dot is an a.c. voltage of frequency Ω_G, the source-drain current oscillates with a higher frequency $\Omega_{sd} = N_g\Omega_G$, where N_g is the number of levels in the big dot which are scanned during one period. In technical terms, one may say that the lateral double-dot device works as a voltage-controlled transistor oscillator, with the property of frequency multiplication.

V. NON-EQUILIBRIUM CONDUCTANCE: ZERO-BIAS ANOMALIES AND SCALING PROPERTIES IN THE KONDO REGIME

It is known that a bias V applied on a single quantum dot in the Kondo regime suppresses the correlations [27, 28] so that the largest value of the differential conductance occurs at $V = 0$, or in other words, the differential conductance $G(V) = dI/dV$ looks peak-like as function of the bias. In what concerns the side-coupled double-dot system, one expects a peak-like behavior for those values of the gate potential V_g and temperature T, where the system behaves Kondo-like. However we have already mentioned that in some range of $\{V_g, T\}$ the interference strongly compete the correlations. In such a situation, it is reasonable to expect a modified behavior of dI/dV, and a dip-like aspect (i.e.,the enhancement with the increasing bias) cannot be *a priori* excluded. In what follows we shall give plausibility arguments which, together with the numerical results, indicate the presence of a peak-dip crossover of the differential conductance.

Let t_r and t_c be the tunneling amplitude along the two channels and t the amplitude of the total transmittance through the device:

$$|t|^2 = |t_c + t_r|^2 = |t_c|^2 + |t_r|^2 + 2|t_c||t_r|cos(\phi_c - \phi_r) \tag{11}$$

The transmittance $|t_c|$ along the continuous (Kondo) path is controlled by V and T, both parameters killing the correlations at large values, so that at $T < T_K$, one has $d|t_c|/dV < 0$ and also $d|t_c|/dT < 0$. The peak or dip aspect effect is given by the sign of the derivative:

$$\frac{d|t|^2}{dV} = 2\frac{d|t_c|}{dV}\ [|t_c| + |t_r|cos(\phi_c - \phi_r)] \tag{12}$$

Since the sign of $\frac{d|t_c|}{dV}$ is fixed, the enhancement or depletion of the total transmittance with increasing bias depends on the sign of the quantity $A = |t_c| + |t_r|cos(\phi_c - \phi_r)$.

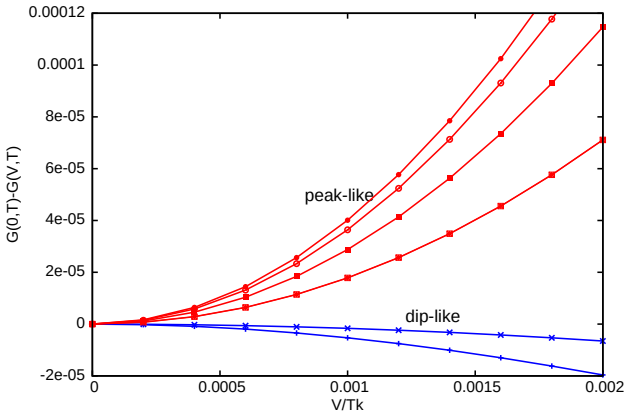


FIG. 6: (color online) $\Delta G(V,T)$ as function of the source-drain bias (scaled with T_K) showing the dip-peak crossover when the gate potential is changed from $V_g/\Delta = -17.00$ (lowest curve) to $V_g/\Delta = -17.70$ (highest curve) at fixed temperature $T = T_K/100$. The small dot is in the Kondo regime $\Gamma/|E_d| = 0.2$.

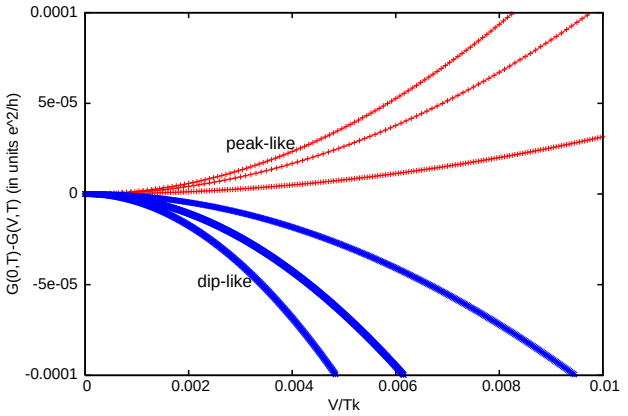


FIG. 7: (color online) $\Delta G(V,T)$ as function of the source-drain bias (scaled with T_K) showing the dip-peak crossover with increasing temperature at fixed gate potential $V_g/\Delta = -17.10$. The lowest curve correspond to $T/T_K = 1/80$ the highest curve to $T/T_K = 1/5$. $\Gamma/|E_d| = 0.4$.

The above expression points out that the dip-like dependence of the transmittance as function of the bias is allowed for values of $\{V_g, T\}$ such that $A < 0$, fact that expresses the implication of phases in this effect. Indeed, the numerical calculations show that the zero bias anomaly may exhibit not only the enhancement but also a depletion of differential conductance depending on the interference conditions. Fig.6 depicts the quantity $\Delta G(V,T) = G(0,T) - G(V,T)$ as function of V for different values of the gate potential V_g at a given temperature. Depending on V_g both the decrease and increase of the source-drain

bias can be noticed.

Let us now keep a fixed gate and use the temperature as the control parameter. This case is exemplified in Fig.7 which shows that also in this situation the conductance undergoes a crossover from dip to peak behavior: the dips occur at low T, and with increasing temperature the conductance dependence on V becomes peak-like.

With the ansatz that $\Delta G(V, T, T_k)$ is a homogeneous function, scaling properties of this function have been studied. For the fully screened Kondo problem of the single dot, Ralph *et al.* [14] suggest that ΔG scales like:

$$\Delta G(V, T) \sim T^{s_1} F(VT^{s_2}) \tag{13}$$

with the exponents $s_1 = 2, s_2 = -1$. A deviation from this law has been observed already in the limit of low-V and low-T by Schiller and Herschfield [13]. Grobis et al [15] describe their experimental data in terms of scaled variables V/T_K and T/T_K by the following expression (eq.(4) in [15]):

$$\frac{\Delta G(V, T)}{c_T G_0} \approx \alpha \big(\frac{V}{T_K}\big)^2 \big[1 - \frac{c_T}{\alpha\gamma}\big(\frac{T}{T_K}\big)^2\big], \tag{14}$$

with universal coefficients along the Kondo plateau, slight variations being observed however in the mixed valence regime. The coefficient α has been calculated also theoretically in Refs.[29, 30].

We look for similar properties in the Fano-Kondo regime of the double dot system. The problem becomes more difficult since, besides the variables V, T and the parameters describing the Kondo dot (packed into the Kondo temperature T_{K0} of the SIAM), the function ΔG depends also on the parameters that describe the state of the side-dot. It is obvious that the SIAM Kondo temperature T_{K0} is no longer a suitable scaling parameter. We need a scaling parameter -an effective Kondo temperature T_K- that accounts also for the spectral influence of the side-coupled dot. This Kondo temperature will depend on V_g. In addition, since the system may shift from peak to dip behavior (as proved in Figs.6-7), it seems impossible to find a unique scaling law describing both the peak and dip regions. It remains however a legitimate task to seek scaling properties in the regions with Kondo behavior along the Fano line. In Fig.8a the arrows indicate four values of the gate V_g for which we test the scaling law (in all these points the non-equilibrium conductance behaves peak-like; the dip-type dependence occurs only in a narrow vicinity of the Fano zero). In other words, we check whether the function $\Delta G(V, T)$ may be scaled in terms of the variables V/T_K and T/T_K. A

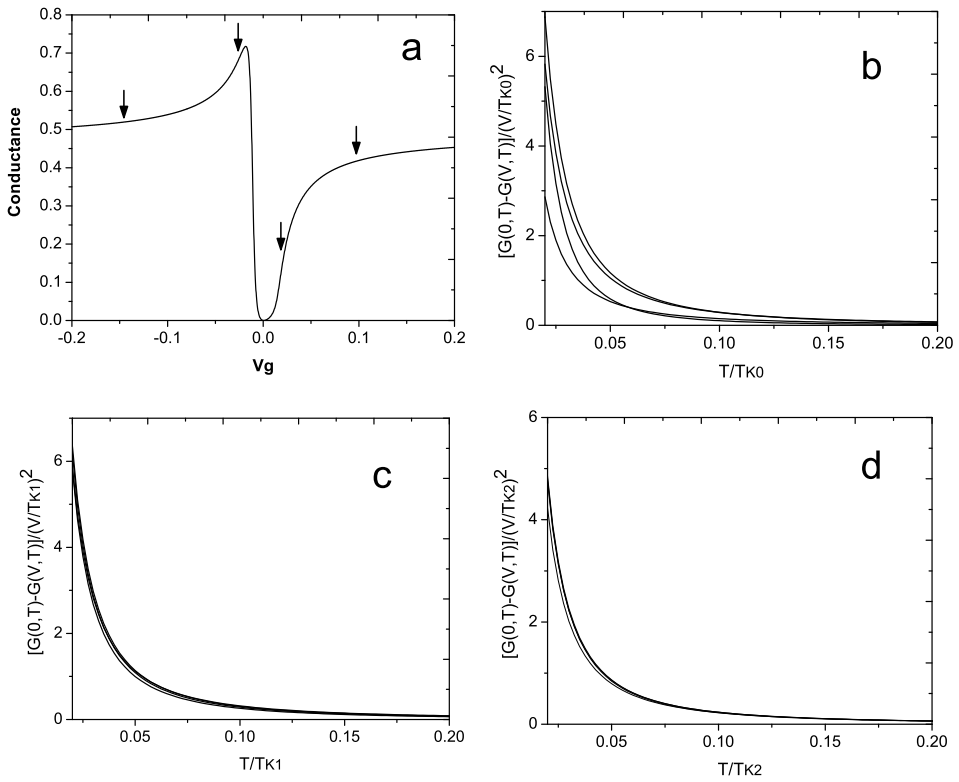


FIG. 8: a) A Fano-Kondo line. The arrows indicate four values of Vg (form left to right: -0.15, -0.03, 0.03 and 0.1) for which ΔG is plotted. Three definitions are considered for the Kondo temperature: b) The SIAM Kondo temperature T_{K0}, which does not depend on Vg, c) The half-width of the Kondo peak at $T = 0$, as estimated in [20] - T_{K1}. d) The half-width of the Kondo peak at a finite temperature, calculated as described in text - T_{K2}. In both cases c) and d) the Kondo temperature depends on Vg, and the scaling is satisfactory, resulting in the data collapse. For all curves, $V = T_K/100$.

quadratic dependence on the bias can be assumed from the start, as we work in the limit of low bias and therefore it is legitimate to keep only the quadratic term. The V^2 dependence of ΔG is visible also in Figs.6-7.

Fig.8 shows the function $\Delta G/(V/T_K)^2$ plotted versus T/T_K for different definitions of T_K in order to see if the data collapse occurs. In Fig.8b we use T_{K0} (the SIAM Kondo temperature) and, as expected, the collapse of the curves (corresponding to the four values of V_g) fails.

Then we check two other possible definitions for the effective T_K. The first (referred as

T_{K1}) is that one proposed in [20] where T_{K1} was calculated as the half-width of the Kondo resonance at $T = 0$ and deep level regime. Using simplifying assumption, the authors obtained an analytical expression (eq.60). By using T_{K1}, our curves fall on top of each other with a precision of a few percents. The situation is plotted in Fig.8c.

Keeping in mind the difficulties to reach numerically the $T = 0$ limit, we calculate also the half-width of the Kondo resonance at a low but finite temperature T=Tk/100 (which we call T_{K2} [31]). This proves also a suitable scaling parameter, leading to the data collapse in Fig.8d.

Two comments are necessary:

1. We have looked for the scaling parameter in two different ways corresponding in fact to two different estimates of the Kondo temperature defined as the half-width of the Kondo resonance in DoS. The important thing is that T_{K1} and T_{K2} vary *in the same way* at the change of the system parameters, and the ratio of the two remains roughly constant $T_{K2}/T_{K1} \in [0.11, 0.14]$.

2. The EOM is an approximate method and this may be responsible for the slight imprecision in the fit of the scaled curves, and also for shape of the scaling function which has the correct decreasing behavior, but is not quadratic as predicted by [13] (however, that prediction regards the SIAM, and not the Fano-Kondo set-up).

VI. CONCLUSIONS

Recently, Sasaki *et.al.*[1] proposed a new set-up for the study of the Fano-Kondo effect: a Kondo dot is directly coupled to conducting leads and a second dot (assumed non-interacting) is side-coupled to the Kondo dot. The set-up mimics a transistor, where the side-dot plays the role of the basis, and whose functionality is controlled by the level of the Kondo correlations, but also by the interference processes.

Due to the many-level aspect of the big dot, the source-drain current presents oscillations with Fano profile when the gate is varied continuously. In the Kondo regime, the Fano lines become more asymmetric as the temperature decreases (in concordance with [1]) corresponding to the increase of the Kondo direct transmission. The Fano dip always reaches *zero* conductance, as resulting also with the slave boson method [5, 6].

The new physics is interesting since the strong hybridization of the dots has a significant

influence on the Kondo effect. In the vicinity of the Fano zero, the Kondo effect is strongly suppressed and the conductance varies negligibly with the temperature. Moreover, in this regime, the destructive interference leads to a *zero* bias dip-type anomaly in the differential conductance. Outside this region, the differential conductance shows the expected peak behavior.

Interestingly, the non-equilibrium conductance exhibits scaling properties similar to the SIAM, even in the presence of the Fano interference. Nevertheless, the SIAM Kondo temperature is no more the suitable scaling parameter. Provided we are in the low bias and low temperature domain, the function $\Delta G = G(0,T) - G(V,T)$ calculated for different values of V_g, depends *only* on V/T_K and T/T_K, where the scaling invariant T_K is extracted from the half-width of the Kondo peak in DoS_d of the double dot.

We have used the Keldysh transport formalism and the equation of motion method which captures not only the Kondo spin fluctuations but also the charge fluctuations, an important ingredient for the aspect of the Fano-Kondo resonances.

In a very recent paper, Balseiro *et. al.* [32] also show that the EOM method is suitable for checking scaling properties in the Kondo regime. However they address the SIAM, and not the Fano-Kondo set-up.

VII. ACKNOWLEDGEMENTS

We acknowledge support from PNCDI2-Research Programme (grant no 515/2009), Core Programme (contract no.45N/2009) and Sonderforschungsbereich 608 at the Institute of Theoretical Physics, University of Cologne. One of the authors (AA) is very much indebted to R.Bulla and E.Sela for illuminating discussions.

---

[1] S. Sasaki, H. Tamura, T. Akazaki, and T. Fujisawa, Phys.Rev.Lett. **103**, 266806 (2009).

[2] P.S. Cornaglia and D.R. Grempel, Phys.Rev.B **71**, 075305 (2005).

[3] C.H. Chung, G. Zarand, and P. Wölfle, Phys.Rev.B **77**, 035120 (2008); C.H. Chung and T.H. Lee, Phys.Rev.B **82**, 085325 (2010).

[4] B.H. Wu, J.C. Cao, and K.-H. Ahn, Phys.Rev.B **72**, 165313 (2005).

[5] H. Tamura, S. Sasaki, Physica E **42**, 864 (2010).

[6] Y.S. Liu, X.F. Yang, X.H. Fan and Y.J. Xia, J.Phys.:Condens.Matter **20**, 135226 (2008).

[7] R. Zitko, Phys.Rev.B **81**, 115316 (2010).

[8] I. Weymann and J. Barnas,Phys.Rev.B **81**, 035331 (2010).

[9] B.I. Shklovskii and A.L. Efros, Electronic Properties of Doped Semiconductors, Springer Verlag (1984), p. 228.

[10] B.L. Altshuler and A.G. Aronov, Electron-Electron Interaction In Disordered Conductors, Elsevier Science Publishers B.V., (1985), p.46.

[11] J. König, J. Schmid, H. Schoeller, and G. Schön, Phys.Rev.B **54**, 16820 (1996).

[12] D. Goldhaber-Gordon, H. Shtrikman, D. Mahalu, D. Abusch-Megder, U. Meirav, and M.A. Kastner, Nature **391**, 156 (1998).

[13] A. Schiller and S. Hershfield, Phys.Rev.B **51**, 12896 (1995).

[14] D.C. Ralph, A.W.W. Ludwig, J. von Delft, and R.A. Buhrman, Phys.Rev.Lett. **72**, 1064 (1994).

[15] M. Grobis, I.G. Rau, R.M. Potok, H. Shtrikman, and D. Goldhaber-Gordon, Phys.Rev.Lett. **100**, 246601 (2008).

[16] A. Oguri, Phys.Rev.B, **64**, 153305 (2001).

[17] G.D. Scott, Z.K. Keane,J.W. Ciszek, J.M. Tour, and D. Natelson Phys.Rev.B, **79**, 165413 (2009).

[18] K. Majumdar, A. Schiller, and S. Hershfield, Phys.Rev.B **57**, 2991 (1998).

[19] Y. Meir, N.S. Wingreen, and P.A. Lee, Phys.Rev.Lett **70**, 2601 (1993).

[20] O. Entin-Wohlman, A. Aharony, and Y. Meir, Phys.Rev. B **71**, 035333 (2005).

[21] C. Lacroix, J. Phys. F: Metal Phys. **11**, 2389 (1981).

[22] M. Ţolea, I.V. Dinu, and A. Aldea, Phys.Rev.B **79**, 033306 (2009).

[23] I.V. Dinu, M. Ţolea, and A. Aldea, Phys.Rev.B **76**, 113302 (2007).

[24] W.B. Thimm, J. Kroha, and Jan von Delft, Phys.Rev.Lett. **82**,2143(1999).

[25] P. Simon, J. Salomez, and D. Feinberg, Phys. Rev. B **73**, 205325 (2006).

[26] R.K. Kaul, D. Ullmo, G. Zarand, S. Chandrasekharan, and H.U. Baranger, Phys. Rev. B **80**, 035318 (2009).

[27] N.S. Wingreen and Y. Meir, Phys.Rev.B **49**, 11040 (1994).

[28] J. Paaske, A. Rosch, J. Kroha, and P. Wölfle, Phys.Rev.B **70**, 155301 (2004).

[29] E. Sela and J. Malecki, Phys.Rev.B **80**, 233103 (2009).

[30] C. Mora, P. Vitushinsky, X. Leyronas, A.A. Clerk, and K. Le Hur, Phys.Rev.B **80**, 155322 (2009).

[31] T_{K2} is calculated by solving numerically the equation $ImG(Ef + T_{K2}/2) = 1/2ImG(Ef)$, at T=TK2/100, after the background is removed (the background is the value of the density of states at a high temperature, when the Kondo peak is absent).

[32] C.A. Balseiro, G. Usaj, M.J. Sanchez, J.Phys.: Condens. Matt. **22**, 425602, (2010).